Available online at www.sciencedirect.com

SCIENCE DIRECT®

Tectonophysics 387 (2004) 189–203

TECTONOPHYSICS

www.elsevier.com/locate/tecto

Azimuthal variation of *Pg* velocity in the Moldanubian, Czech Republic: observations based on a multi-azimuthal common-shot experiment

Václav Vavryčuk[a,*], Pavla Hrubcová[a], Milan Brož[b], Jiří Málek[b]
The ALP 2002 Working Group[1]

[a]Geophysical Institute, Academy of Sciences of the Czech Republic, Boční II, 141 31 Praha 4, Czech Republic
[b]Institute of Rock Structure and Mechanics, Academy of Sciences of the Czech Republic, V Holešovičkách 41, 182 09 Praha 8, Czech Republic

Received 25 September 2003; accepted 23 June 2004

Abstract

We study the azimuthal velocity variation of *Pg* waves in the Moldanubian, which is a crystalline segment within the Bohemian Massif in the Czech Republic. We use the data from a multi-azimuthal common-shot experiment performed as part of the ALP 2002 refraction experiment, complemented by profile refraction data from the CELEBRATION 2000 experiment. We analyze the travel times of waves recorded by 72 portable seismic stations deployed along two circles with radii of 35 and 45 km around a shot. The observed travel times display an azimuthal variation indicating anisotropy of 2%. The minimum and maximum velocity values are 5.83 and 5.95 km/s, respectively. The direction of the maximum velocity is ~N50°E. These values characterize horizontal anisotropy of the uppermost crust down to 3 km. The strength and orientation of uppermost crustal anisotropy in the Moldanubian is consistent with the overall upper crustal anisotropy in the entire Bohemian Massif. The high-velocity direction is roughly perpendicular to the present-day maximum compressive stress in the Bohemian Massif and Central Europe and coincides with the orientation of structures formed by the main Variscan tectonic events in the area. This indicates that the anisotropy is caused predominantly by alignment of textural elements and minerals in the rocks, which developed in early geological stages

* Corresponding author. Fax: +420 272761549.
E-mail address: vv@ig.cas.cz (V. Vavryčuk).

[1] E. Brűckl (Institute of Geodesy and Geophysics, Vienna University of Technology, Austria), coordinator, T. Bodoky (Eötvös Loránd Geophysical Institute, Budapest, Hungary), A. Gosar (Ministry for Environment and Spatial Planning, Environmental Agency of the Republic, Slovenia), M. Grad (Institute of Geophysics, University of Warsaw, Poland), A. Guterch (Institute of Geophysics, Polish Academy of Sciences Warsaw, Poland), Z. Hajnal (Department of Geological Sciences, University of Saskatchewan, Canada), E. Hegedűs (Eötvös Loránd Geophysical Institute, Budapest, Hungary), P. Hrubcová (Geophysical Institute, Academy of Sciences of the Czech Republic, Prague, Czech Republic), G.R. Keller (Department of Geological Sciences, University of Texas at El Paso, USA), A. Špičák (Geophysical Institute, Academy of Sciences of the Czech Republic, Prague, Czech Republic), F. Sumanovac (Faculty of Mining, Geology and Petr. Eng., University of Zagreb, Croatia), H. Thybo (Geological Institute, University of Copenhagen, Denmark), F. Weber (Austrian Academy of Sciences, Vienna, Austria).

doi:10.1016/j.tecto.2004.06.015

rather than by a preferred orientation of cracks or microcracks due to present-day stress. If the crack-induced anisotropy is present in the medium, then its strength should not exceed 1% and the cracks should be water saturated.

Keywords: Anisotropy; Bohemian Massif; Continental crust; Moldanubian; *Pg* waves

1. Introduction

The Earth's crust is often reported to be anisotropic (Babuška and Cara, 1991), which is manifested by azimuthally dependent velocities of seismic waves. Crustal anisotropy in the Bohemian Massif and adjacent areas has so far been measured on rock samples from West Bohemia and from the KTB drill hole (Kern and Schmidt, 1990; Kern et al., 1991; Jahns et al., 1996; Berckhemer et al., 1997; Pros et al., 1998; Martínková et al., 2000; Chlupáčová et al., 2003), from shear-wave splitting observed in records of micro-earthquakes in West Bohemia (Vavryčuk, 1993, 1995) and from shear-wave splitting observed in the VSP records at the KTB site (Rabbel, 1994; Rabbel and Mooney, 1996). The experiments indicate anisotropy of varying magnitude dependent on the site studied. The orientation of anisotropy axes from in situ experiments is rather stable being related to the direction of the horizontal tectonic stress in the region. A similar observation is reported by Plomerová et al. (1981, 1984), who studied a velocity variation of *Pg* waves in the Bohemian Massif from earthquake data. Recently, Růžek et al. (2003) studied a regional-scale upper crustal anisotropy in the Bohemian Massif from *Pg* refraction data collected during the large-scale refraction experiment CELEBRATION 2000 (Guterch et al., 2001, 2003; Málek et al., 2001). They report a systematic azimuthal variation of the *Pg* velocity, indicating an overall anisotropy of 1.5–2.5% with the direction of the maximum propagation velocity in azimuth of ~N35°E. This direction is approximately perpendicular to the direction of the maximum horizontal compression in the earth crust in Central Europe.

Knowing the multisegmental nature of the Bohemian Massif, we wanted to choose just one segment of the Massif in this paper, and study the anisotropy on the local scale. Therefore, we continue the work of Růžek et al. (2003) but study the azimuthal variation of *Pg* waves in the Moldanubian, a crystalline segment of the Bohemian Massif. The aim is to trace a more detailed anisotropy pattern within the Bohemian Massif and to check whether anisotropy of *Pg* waves can be detected even at a local scale. We use data from a multi-azimuthal common-shot experiment performed within the European refraction experiment ALP 2002 (Brückl et al., 2003). A circular geometry of the experiment was chosen to provide an unequivocal check of seismic anisotropy in the studied area. Additionally, we use data from the CELEBRATION 2000 experiment related to the region of interest to obtain more information on velocity distribution in study area and possible heterogeneity corrections.

2. Geological and tectonic setting

The Moldanubian represents a major crystalline segment within the Bohemian Massif, which is one of the largest stable outcrops of pre-Permian rocks in Central Europe, forming the easternmost part of the Variscan Belt. The Bohemian Massif developed approximately between 500 and 250 Ma during a stage of large-scale crustal convergence, collision of continental plates and microplates, and possibly also subduction (Matte et al., 1990), and is subdivided into various units: Saxothuringian, Barrandian, Moldanubian, and Moravo-Silesian (see Fig. 1).

The Moldanubian unit, sometimes viewed as a Precambrian orogenic root surrounded by younger complexes, adjoins the Saxothuringian in the NW and the Moravo-Silesian to the east. The boundary with the Saxothuringian is regarded as a major suture-type discontinuity, whereas the structurally higher unit in the NW, the Barrandian, has been thrust over the Saxothuringian and Moldanubian units. The Moldanubian unit is separated from the Barrandian unit by a major NE–SW trending Variscan dextral fault, the Central Bohemian Shear Zone, which is obscured by

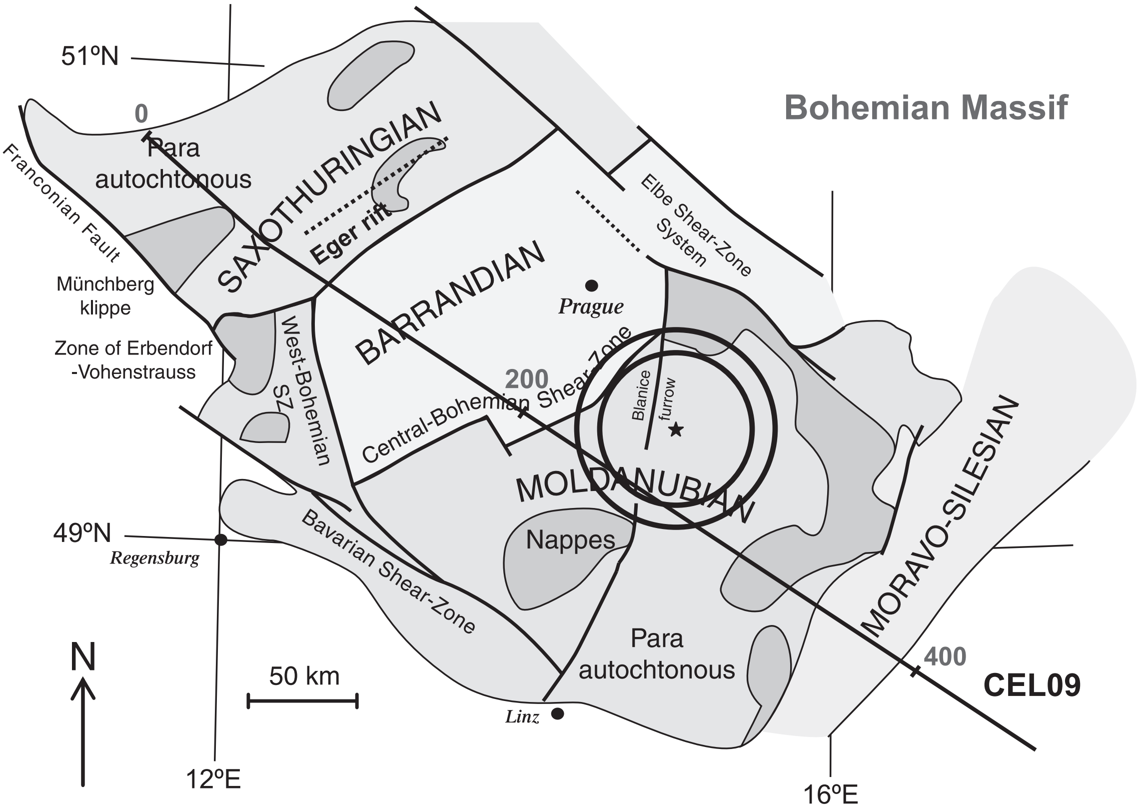

Fig. 1. Major tectonic units of the Bohemian Massif, after Pitra et al. (1999).

Variscan intrusions of the Central Bohemian Pluton. Its eastern boundary with the Moravo-Silesian has the character of a major NE–SW striking ductile shear zone, with a predominance of strike-slip movements. Post-Variscan platform sediments cover the continuation of the Moldanubian unit to the S and SW, where it is bounded by the fault system of the Franconian Line, representing the foreland deformation of the Alpine collision (Dallmeyer et al., 1995).

The Moldanubian segment contains mainly high-grade gneisses and migmatites of supracrustal origin, orthogneisses, granulites, and also numerous Variscan post-tectonic granitoid intrusions, the most prominent of which are the Central Bohemian and Central Moldanubian Plutons. The crustal root of the Moldanubian unit shows nearly vertical NE–SW trending fabrics (estimated age 370–330 Ma) developed mostly in granulites and associated mantle slivers (Schulmann et al., 2002). In detail, the Moldanubian is characterized by an almost missing sedimentary cover except for two small basins filled with Cretaceous and Tertiary sediments in the SSW.

3. Data

A multi-azimuthal common-shot experiment was performed on the territory of the Czech Republic as part of the ALP 2002 refraction experiment in June 2002. A total of 72 one-component seismic stations were deployed along two concentric circles with radii of 35 and 45 km with an angular step of 10° between stations and 5° angular intercircle shift (see Fig. 2). The radii of circles were delimited both geographically by the extent of the Moldanubian and by the resolution of the method applied. A charge of 500 kg of explosives was detonated at the center of the circles at 49.50493°N latitude, 14.94982°E longitude, and 538-m altitude. The positions of the shot and stations were determined by GPS with an accuracy

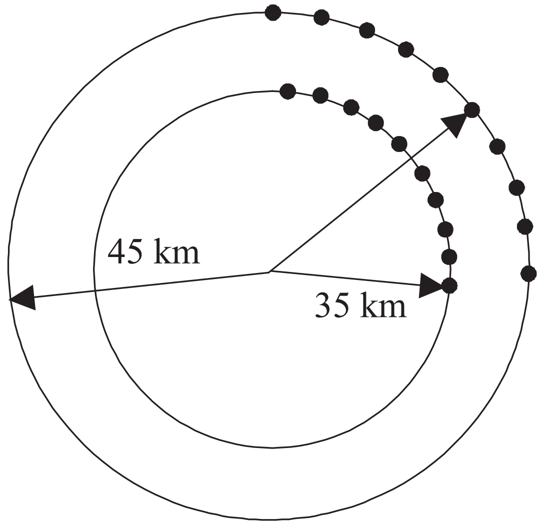

Fig. 2. Geometry of the experiment. Dots mark positions of stations in the azimuth range 0–95°.

better than 20 m; the origin time was controlled by a DCF77 timer with an accuracy of 3 ms. The sensors were 4.5-Hz geophones; the recording instruments were TEXAN.

Fig. 3 shows the *Pg*-wave recordings at the stations. Of the total number of 72 stations, two stations did not record; recordings from four other stations were too noisy to be analyzed. Hence, we analyzed recordings of 66 stations. The sampling frequency of the recordings was 250 Hz. The corner frequency of the anti-alias FIR filter was 100 Hz. The arrival times of *Pg* waves (see Tables 1 and 2) were measured with an accuracy of around 10 ms. The arrival times of *Sg* waves were not analyzed because of high uncertainties in picking in one-component recordings. Fig. 4 shows the azimuthal variation of the *Pg* velocity calculated as distance from the shot divided by travel times. The mean value of the *Pg* velocity is 5.86/5.87 km/s for the inner/outer circle with a standard deviation of 0.06/0.04 km/s.

The calculated velocities show that the crust is not homogeneous or isotropic because the velocity variation is beyond the uncertainty of the measurements. The variation shows the same trend for both circles: It is characterized by high-velocity values for azimuths of 30–60° and by low-velocity values for azimuths of 170–220°. A distinct velocity increase has also been detected for azimuths of 320–360° at the inner circle, but the corresponding velocities at the outer circle display a different and more complicated pattern. The velocity variation indicates either lateral inhomogeneities or anisotropy in the area. As seen from a detailed geological map of the area (see Fig. 5), some of the velocity anomalies can be readily explained by lateral inhomogeneities. This refers, for example, to a rather high scatter of velocities in the NW to N directions, where the circles exceed the Moldanubian and touch or hit the fragmented structure of the Central Bohemian Shear Zone. Local inhomogeneities can also explain the low velocities in the SSW direction, because the stations were located at or very close to the Tertiary Třeboň Basin characterized by an anomalously low-velocity subsurface layer. Therefore, to assess potential overall anisotropy in the area, we have to first eliminate the subsurface inhomogeneity effects.

4. Station corrections

To eliminate the local inhomogeneities from travel times, we can use the CEL09 profile data collected during the CELEBRATION 2000 experiment (Růžek et al., 2003). This profile intersects both circles and traverses different types of the subsurface structure in the region under study. The profile data can be used to address two points: (1) to approximate the depth extent of rays in the experiment, and (2) to calculate station corrections along the profile, corresponding to delay times induced by a low-velocity subsurface layer. The station corrections along the profile can be used to roughly approximate the station corrections along the circles.

Fig. 6 shows the reduced travel times along the profile in the longitude range of 14–15.5° and at distances between 10 and 100 km. Interpolating upper and lower bounds of the travel times by piecewise linear functions, we can infer 1-D layered models (Shearer, 1999, Fig. 5.5), which are limits for the model in the area (see Fig. 7). The limits should reflect lateral inhomogeneities along the profile. The inferred limits differ down to 8 km, and then they coalesce. This manifests a variability of structure in shallow rather than deep parts of the upper crust. The limits also determine the range of the maximum

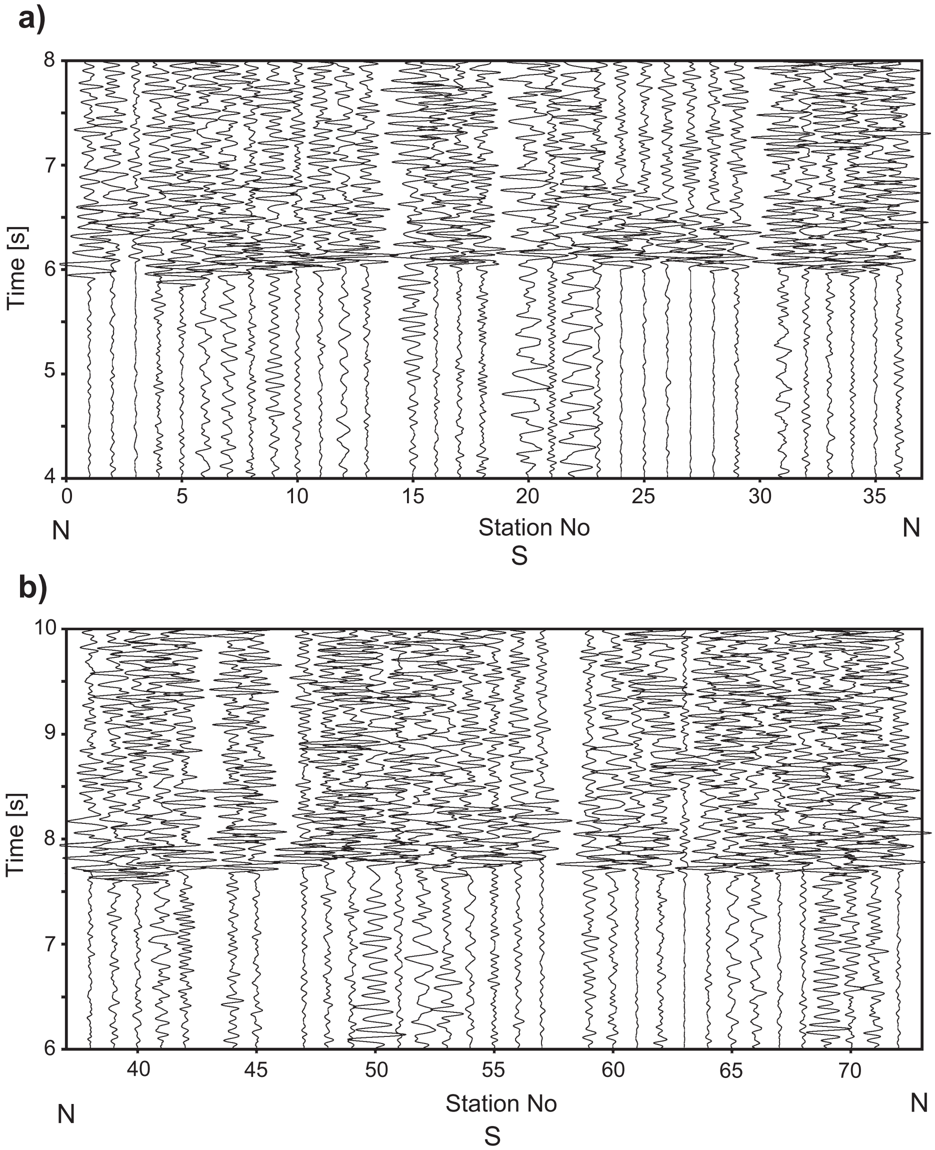

Fig. 3. *Pg*-wave velocity recordings at portable stations deployed along (a) the inner circle at a recording offset of 35 km, and (b) the outer circle at a recording offset of 45 km.

depths reached by rays in the experiment. Fig. 7 shows that the depth is well constrained ranging between 2 and 3 km.

More detailed information on lateral inhomogeneities along the profile can be gained from time station corrections evaluated using the "time-term method" (Bamford, 1977; Enderle et al., 1996; Song et al., 2001). In this method, the measured travel times are corrected for the delay times due to a low-velocity subsurface layer. The thickness and velocity of the layer can significantly vary within the area and are considered to be unknown. The aim is to isolate and remove these unknown effects from the travel times. The station corrections were calculated using the travel times of the *Pg* waves generated by six shots (Table 3) and measured at 73 stations along the

Table 1
The multi-azimuthal experiment: inner circle

No.	Latitude [°N]	Longitude [°E]	H [m]	D [km]	Azimuth [deg]	T [s]	Type of rock	dt [s]	T^{corr} [s]	Velocity [km/s]
1	49.8131	14.9510	387	34.27	0.1	5.878	B, D	−0.05	5.928	5.78
2	49.8145	15.0347	472	34.97	10.1	6.043	B	0.00	6.043	5.79
3	49.8022	15.1183	510	35.23	20.1	6.058	B	0.00	6.058	5.82
4	49.7786	15.1883	407	34.97	29.4	5.914	B	0.00	5.914	5.91
5	49.7459	15.2640	480	35.12	40.1	5.846	B	0.00	5.846	6.01
6	49.7062	15.3237	515	35.09	50.2	5.924	B	0.00	5.924	5.92
7	49.6599	15.3691	425	34.88	60.2	5.908	A	0.00	5.908	5.90
8	49.6112	15.4054	540	35.02	70.1	5.970	A	0.00	5.970	5.87
9	49.5584	15.4245	600	34.88	80.0	5.920	A	0.00	5.920	5.89
10	49.5039	15.4338	615	35.05	90.0	5.989	A	0.00	5.989	5.85
11	49.4479	15.4215	635	34.76	100.3	5.947	A	0.00	5.947	5.85
12	49.3957	15.4042	632	35.12	110.1	6.014	A	0.00	6.014	5.84
13	49.3471	15.3666	592	34.96	120.0	6.015	A	0.00	6.015	5.81
15	49.2637	15.2590	620	34.98	140.0	6.008	A	0.00	6.008	5.82
16	49.2314	15.1901	620	35.08	150.1	6.003	A	0.00	6.003	5.84
17	49.2098	15.1141	555	34.93	160.0	6.003	A	0.00	6.003	5.82
18	49.1967	15.0341	502	34.83	169.8	6.022	A	0.00	6.022	5.78
19	49.1898	14.9495	548	35.04	180.0	6.054	A	0.00	6.054	5.79
20	49.1940	14.8661	460	35.11	190.0	6.049	A	0.00	6.049	5.80
21	49.2094	14.7850	453	34.98	200.1	6.077	C	0.08	5.997	5.83
22	49.2322	14.7098	415	34.98	210.0	6.049	C	0.08	5.969	5.86
23	49.2615	14.6369	443	35.34	220.1	6.040	C	0.10	5.940	5.95
24	49.3022	14.5810	478	35.00	230.0	5.967	C	0.10	5.867	5.96
25	49.3464	14.5310	468	35.13	240.0	5.950	C	0.08	5.870	5.98
26	49.3950	14.4927	473	35.33	249.9	6.027	C	0.08	5.947	5.94
27	49.4491	14.4732	517	35.10	260.0	5.973	B	0.00	5.973	5.88
28	49.5036	14.4668	580	34.99	269.9	5.944	D	−0.05	5.994	5.84
29	49.5585	14.4727	580	35.05	280.0	5.982	D	−0.05	6.032	5.81
31	49.6611	14.5287	495	35.06	299.9	5.998	D	−0.05	6.048	5.80
32	49.7068	14.5762	440	35.12	309.9	5.985	D	−0.05	6.035	5.82
33	49.7454	14.6368	380	35.02	319.9	5.934	D	−0.05	5.984	5.85
34	49.7770	14.7066	365	34.99	330.0	5.879	D	−0.05	5.929	5.90
35	49.8005	14.7830	465	35.01	339.9	5.903	D	−0.05	5.953	5.88
36	49.8143	14.8653	350	34.95	350.0	5.926	D	−0.05	5.976	5.85

Meaning of quantities: No. is the station number, H is the altitude, D is the distance, T is the travel time, dt is the station correction, $T^{corr}=T-dt$ is the travel time corrected for the local geology. Types of geological units at the locations of the individual seismic stations: (A) granitoid intrusions of the Central Moldanubian Pluton (station nos. 7–20, 49–54); (B) high-grade gneisses and migmatites, orthogneisses, granulites with intrusions of amphibolites (station nos. 1–6, 27, 38–48, 62); (C) Tertiary and Quaternary sediments (station nos. 21–26, 55–61); (D) granitoid plutons (station nos. 28–36, 63–64); (E) granitoid plutons with mafic intrusions (amfibolites, diabases, melaphyres) of Central Bohemian Pluton (station nos. 65–71); (F) Palaeozoic sediments (station no. 72).

profile with longitudes in the range of 13–15.5°E. We selected stations with the recording offset between 30 and 150 km. On the whole, 245 travel times were inverted for 73 station and six shot corrections.

The station corrections vary from −0.10 to 0.12 s (Fig. 8) and display systematic trends, which correlate with the geological structure along the profile (see Fig. 5). The studied segment of the CEL09 profile intersects with the contact between the Barrandian in the NW and the Moldanubian (Central Bohemian Shear Zone) and continues across the Moldanubian to the SE. High corrections (low velocities) at longitude 13.6°E are connected with Barrandian Palaeozoic sediments and metasediments (type F). The low corrections (high velocities) at 13.8–14.1°E relate to granitoid plutons with mafic intrusions (amfibolites, diabases, melaphyres) at the

Table 2
The multi-azimuthal experiment: outer circle

No.	Latitude [°N]	Longitude [°E]	H [m]	D [km]	Azimuth [deg]	T [s]	Type of rock	dt [s]	T^{corr} [s]	Velocity [km/s]
38	49.8953	15.1116	448	44.96	15.0	7.676	B	0.00	7.676	5.86
39	49.8709	15.2152	420	44.99	25.1	7.579	B	0.00	7.579	5.94
40	49.8342	15.3096	412	44.89	35.2	7.544	B	0.00	7.544	5.95
41	49.7920	15.3914	426	45.13	44.8	7.572	B	0.00	7.572	5.96
42	49.7362	15.4617	493	45.05	55.0	7.668	B	0.00	7.668	5.88
44	49.6076	15.5517	417	45.02	75.1	7.655	B	0.00	7.655	5.88
45	49.5385	15.5717	527	45.18	85.0	7.676	B	0.00	7.676	5.89
47	49.3985	15.5488	548	45.02	105.0	7.696	B	0.00	7.696	5.85
48	49.2703	15.4612	630	45.38	124.9	7.771	B	0.00	7.771	5.84
49	49.2703	15.4619	603	45.42	124.9	7.761	A	0.00	7.761	5.85
50	49.2183	15.3875	639	45.02	134.9	7.706	A	0.00	7.706	5.84
51	49.1731	15.3043	673	45.01	144.9	7.709	A	0.00	7.709	5.84
52	49.1385	15.2112	578	44.97	154.9	7.690	A	0.00	7.690	5.85
53	49.1185	15.1069	533	44.46	165.1	7.603	A	0.00	7.603	5.85
54	49.1025	15.0036	469	44.93	175.0	7.672	A, C	0.05	7.622	5.89
55	49.1024	14.8967	464	44.93	185.0	7.712	C	0.05	7.662	5.86
56	49.1142	14.7892	434	44.99	195.1	7.746	C	0.10	7.646	5.88
57	49.1383	14.6893	425	44.96	205.0	7.784	C	0.12	7.664	5.87
59	49.2183	14.5124	440	45.01	225.1	7.668	C	0.10	7.568	5.95
60	49.2715	14.4399	396	45.21	235.2	7.662	C	0.08	7.582	5.96
61	49.3331	14.3880	446	45.02	245.1	7.676	C	0.05	7.626	5.90
62	49.3988	14.3507	476	45.02	255.0	7.637	B	0.00	7.637	5.89
63	49.4685	14.3319	516	44.95	265.1	7.619	D	−0.05	7.669	5.86
64	49.5386	14.3294	525	45.08	275.0	7.634	D	−0.05	7.684	5.87
65	49.6080	14.3451	465	45.23	284.9	7.605	E	−0.08	7.685	5.89
66	49.6749	14.3838	380	45.08	295.0	7.639	E	−0.08	7.719	5.84
67	49.7356	14.4373	345	45.05	304.9	7.651	E	−0.08	7.731	5.83
68	49.7899	14.5062	440	45.07	314.9	7.694	E	−0.08	7.774	5.80
69	49.8377	14.5877	280	45.31	324.9	7.633	E	−0.08	7.713	5.87
70	49.8706	14.6841	350	44.96	334.9	7.595	E	−0.08	7.675	5.86
71	49.8943	14.7875	420	44.86	344.9	7.689	E, F	0.00	7.689	5.83
72	49.9074	14.8957	400	44.94	355.0	7.663	F	0.05	7.613	5.90

For the meaning of quantities, see the legend of Table 1.

Barrandian/Moldanubian contact (type E), and the low corrections around 14.3°E reflect high-grade gneisses and migmatites, orthogneisses and granulites (type D). The high corrections around 14.5–14.7°E relate to Tertiary and Quaternary sediments of the Třeboň basin (type C). Granitoid intrusions of the Central Moldanubian Pluton (type A) cover the interval 14.8–15.2°E. The high corrections around 15.0°E could reflect a local sedimentary structure (type G). Places with zero corrections represent the Moldanubian unit (gneisses, migmatites, type B) and the granitoid intrusions of the Central Moldanubian Pluton (type A).

Because the station corrections correspond well to the geological structure under the stations, we conclude that the evaluation of effects of the subsurface inhomogeneities was successful and that the travel times along the circles can be effectively corrected for them (see Tables 1 and 2).

5. Anisotropy

A circular geometry of the experiment is particularly suitable for studying anisotropy and eliminating or at least suppressing other inhomogeneity effects not accounted for by station corrections. This concerns, for example, effects caused by varying depth of a low-velocity subsurface layer, differences in velocity gradients, or differences in the depth range sampled

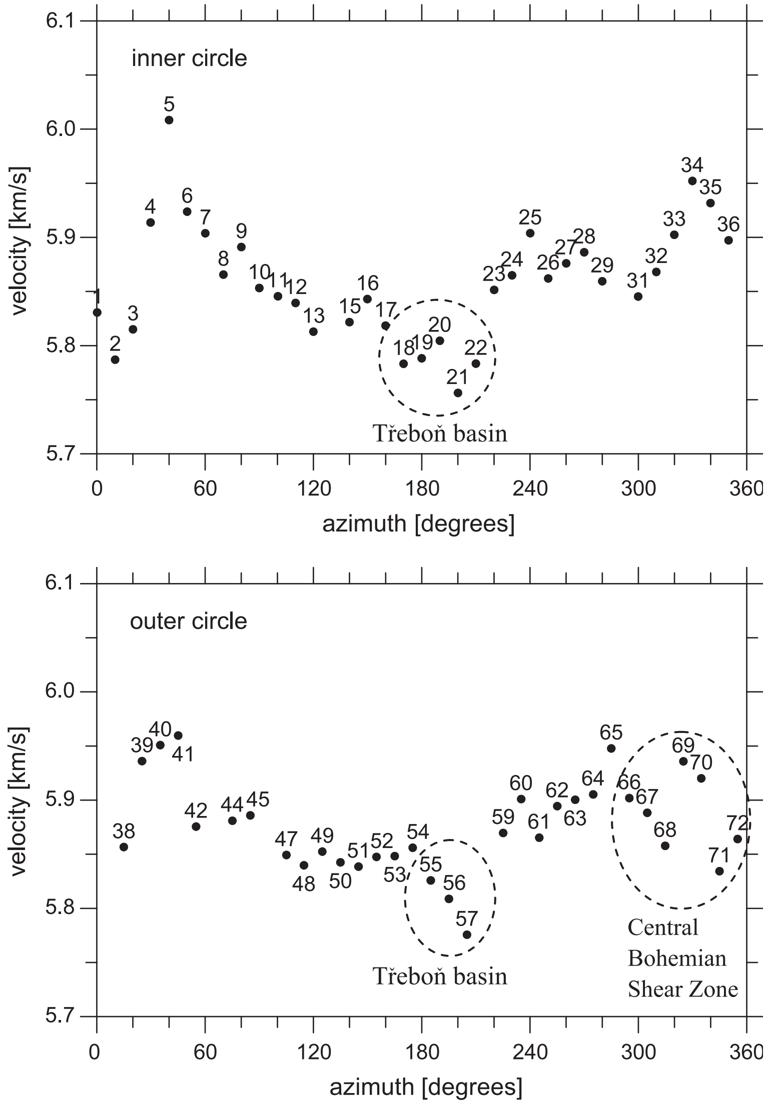

Fig. 4. Uncorrected *Pg* velocity as a function of azimuth for the inner (upper plot) and outer (lower plot) circles.

by the data. To separate anisotropy from the mentioned inhomogeneities, we show the *Pg* velocities calculated from the corrected travel times in the azimuth range 0–180° (Fig. 9). In this range, we compare velocities for the rays being shot in opposite directions and thus sampling different structures. If the velocities retrieved from the opposite rays are consistent and display a pronounced variation with varying azimuth, then it should primarily be the result of anisotropy. The scatter in velocities for the opposite rays quantifies the effects of inhomogeneities not satisfactorily eliminated by applying the station corrections. Fig. 9 shows a distinct azimuthal variation of the *Pg* velocity and a rough coincidence of this variation along both circles. The variation displays two peaks: a distinct maximum in azimuths of 30–60°, and a less distinct maximum around an azimuth of 150°. The azimuthal velocity variation along both circles indicates that the medium is intrinsically or effectively anisotropic.

Assuming mostly horizontal propagation of refracted waves in a weakly anisotropic crust,

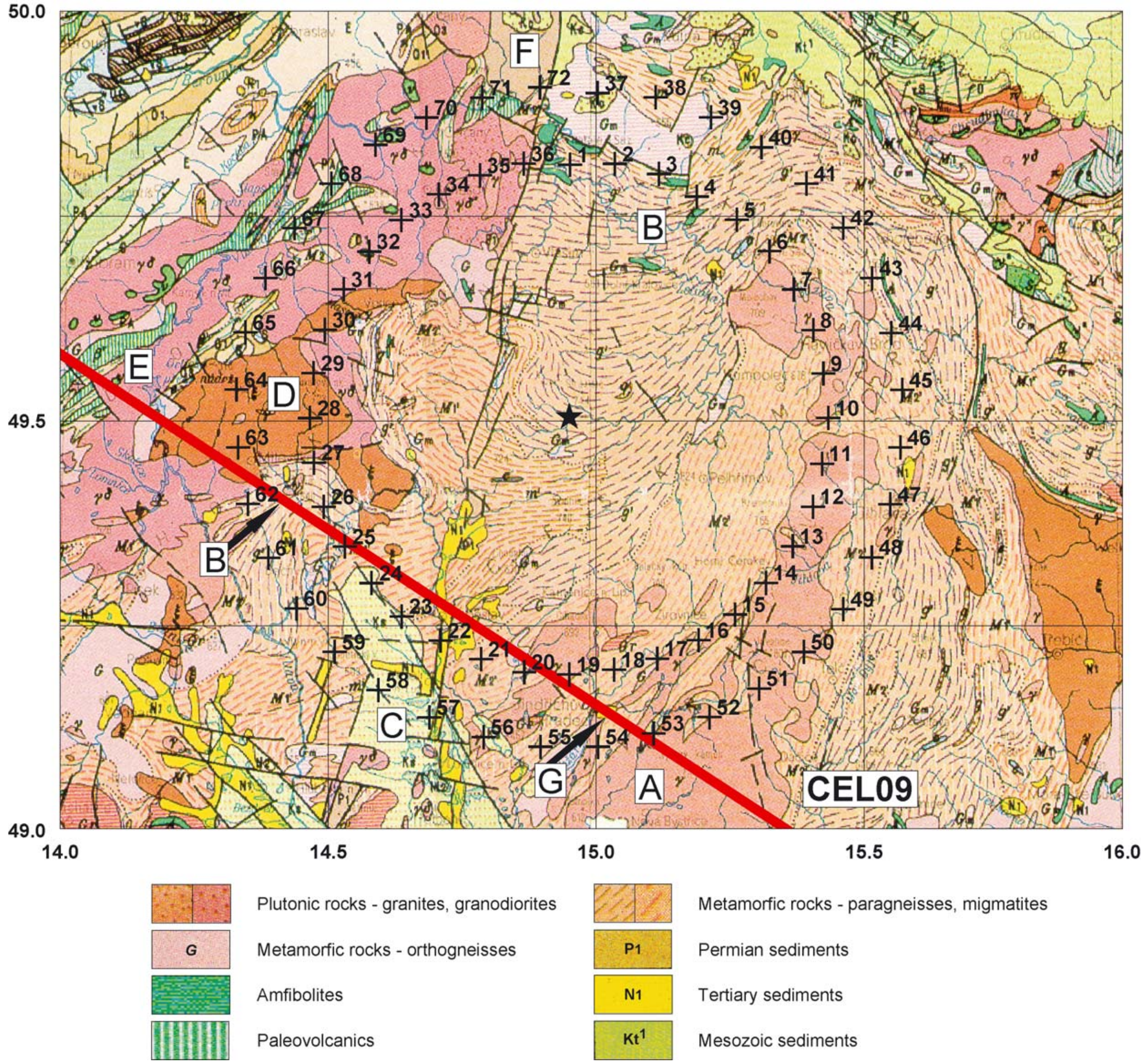

Fig. 5. Geological settings and experiment layout, after Fusán et al. (1993). Crosses mark positions of stations; the star marks the position of the shot.

we can express the velocity as follows (Backus, 1965):

$$v = v_0(1 + A\cos 2\varphi + B\sin 2\varphi + C\cos 4\varphi + D\sin 4\varphi) \tag{1}$$

where v is the azimuth-dependent velocity, v_0 is the velocity in an isotropic reference medium, φ defines the azimuth in which the wave propagates, and constants A, B, C, and D are small unknown coefficients that are linear combinations of the elastic parameters defining weak anisotropy. For weak transverse isotropy with a horizontal axis of symmetry, Eq. (1) simplifies to (Song et al., 2001)

$$v = v_0(1 + E\cos 2(\varphi - \varphi_0) + F\cos 4(\varphi - \varphi_0)) \tag{2}$$

where φ_0 is the angle defining the orientation of the symmetry axis in the horizontal plane, and E and F are small unknown coefficients defining weak transverse isotropy.

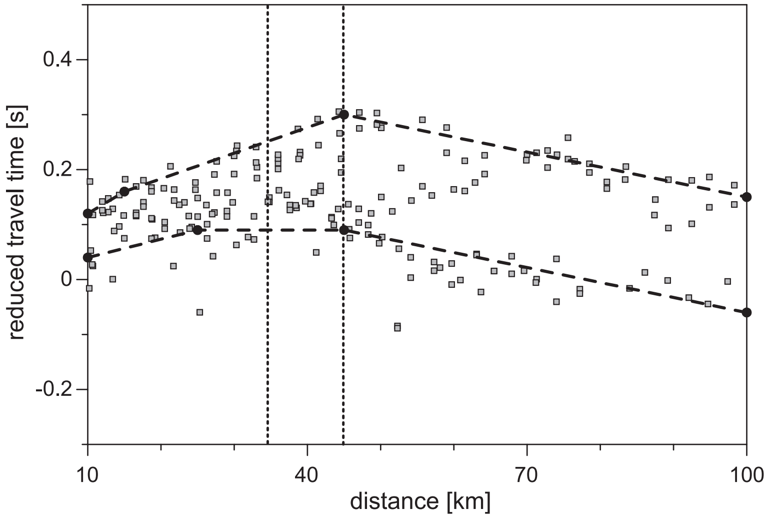

Fig. 6. The reduced travel times along the CEL09 profile as a function of distance. The reduction velocity is 6 km/s. The dashed lines consist of straight-line segments and delineate upper and lower bounds of the travel times. The points between the segments are marked by black dots. Dotted lines show the recording offsets used in the multi-azimuthal common-shot experiment.

Inverting the whole set of the velocity values for an optimum anisotropy model using Eqs. (1) and (2), we obtain v_0=5.87 km/s, A=−0.0019, B=0.0078, C=−0.0044, D=−0.0027, φ_{max}=53°, and ε=2.0% for weak general anisotropy, and v_0=5.87 km/s, E = 0.0082, F=0.0049, φ_{max}=50°, and ε=2.0% for weak transverse isotropy, where φ_{max} is the azimuth of the maximum velocity direction and ε is the strength of anisotropy defined as

$$\varepsilon = 2\frac{v_{max} - v_{min}}{v_{max} + v_{min}}100\% \tag{3}$$

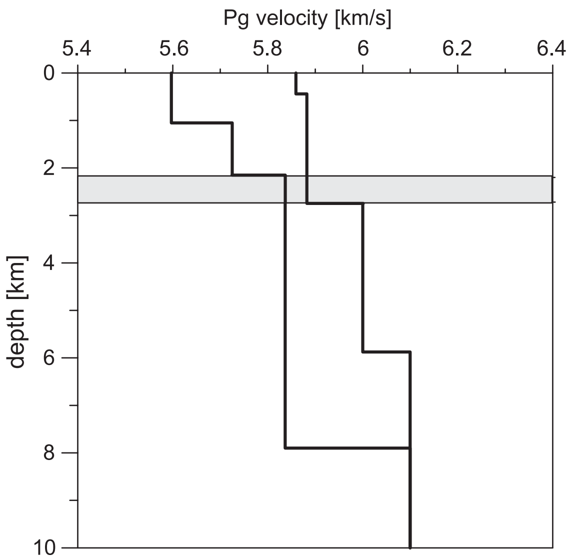

Fig. 7. The 1-D layered models inferred from the travel times along the CEL09 profile in the longitude range 14–15.5°. The shadow area shows the maximum depths reached by rays in the experiment.

The velocity variations for the optimum models of general anisotropy and transverse isotropy are very similar (see Fig. 10, lower plot). They are also very similar to the variations obtained when inverting the data of the east semicircles (see Fig. 10, upper plot). For east semicircles, no station corrections were applied because of the absence of distinct subsurface inhomogeneities (see Fig. 5).

6. Discussion

Růžek et al. (2003) used *Pg* refraction data from the CELEBRATION 2000 experiment to study regional horizontal upper crustal anisotropy in the Bohemian Massif. They used data covering the whole range of azimuths and with recording offsets from 30 to 190 km. They found that the high-velocity direction in the entire Bohemian Massif is ~N35°E, and the overall azimuthal velocity variation is 1.5–2.5%. For studying local scale horizontal anisotropy, we choose the Moldanubian unit, a crystalline segment within the

Table 3
Parameters of the CEL09 shots

Date	Time [hh:mm:ss.sss]	Shot ID	Charge [kg]	H [m]	Latitude [°N]	Longitude [°E]	Territory
Jun 24	21:00:00.000	2-910-0	210	476	49.3124	14.5900	Czech Rep.
Jun 24	22:00:00.000	2-909-0	210	474	49.5182	14.1295	Czech Rep.
Jun 24	22:45:00.000	2-912-0	210	612	49.0191	15.3173	Czech Rep.
Jun 24	23:15:00.000	2-912-1	210	615	49.0191	15.3168	Czech Rep.
Jun 25	00:15:00.000	2-911-0	210	492	49.1892	14.9104	Czech Rep.
Jun 25	00:45:00.000	2-911-1	210	492	49.1896	14.9105	Czech Rep.

Bohemian Massif. Based on a multiazimuthal common-shot experiment with recording offsets 35 and 45 km, we found the horizontal anisotropy strength of 2.0% with the high-velocity direction N50°E. These values characterize anisotropy of the uppermost crust down to 3 km. Hence, we conclude that horizontal anisotropy on a local scale in the Moldanubian unit is consistent with that in the entire Bohemian Massif. This might indicate that the horizontal anisotropy pattern for the uppermost crust is stable with no distinct lateral or vertical variations within the Bohemian Massif.

Interestingly, the fast directions in the Moldanubian unit and in the Bohemian Massif are almost perpendicular to the present-day maximum compressive stress in the region, estimated to be in azimuths of N125–150°E (Peška, 1992). The NW–SE direction of the maximum compressive stress is also reported for the KTB drill hole in Germany (Brudy et al., 1997, azimuth of 160°±10°) and for the overall stress orientation in Western Europe (Müller et al., 1992, azimuth of 144°±26°). Because the high-velocity direction does not coincide with the direction of the present-day maximum compressive stress in the region, we conclude that the observed anisotropy cannot be primarily affected by the presence of cracks or microcracks in the crust (Kaneshima et al., 1988; Crampin, 1994). The dry crack model predicts the maximum Pg velocity in the direction parallel to the maximum compression,

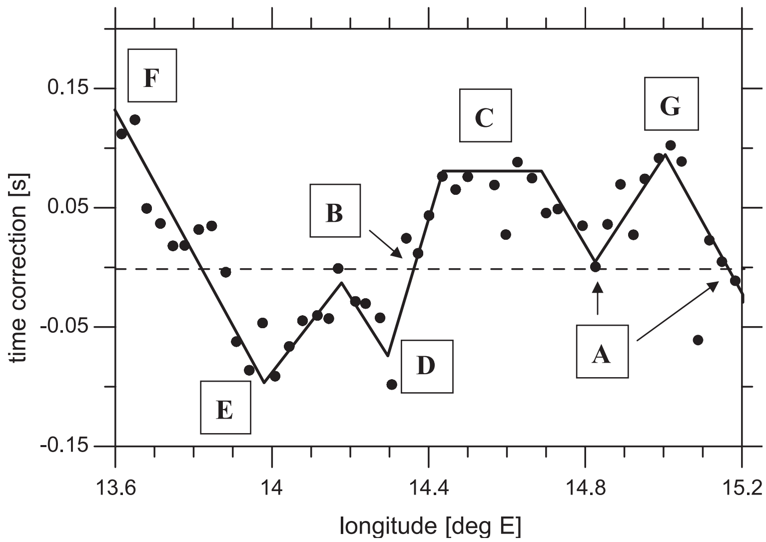

Fig. 8. Station corrections along the CEL09 profile. Types of geological structures: (F) Barrandian Palaeozoic sediments; (E) granitoid plutons with mafic intrusions; (D) granitoid plutons; (B) gneisses and migmatites of the Moldanubian unit; (C) Tertiary and Quarternary sediments (Třeboň basin); (A) granitoid intrusions of the Central Moldanubian Pluton; and (G) local Quarternary sediments.

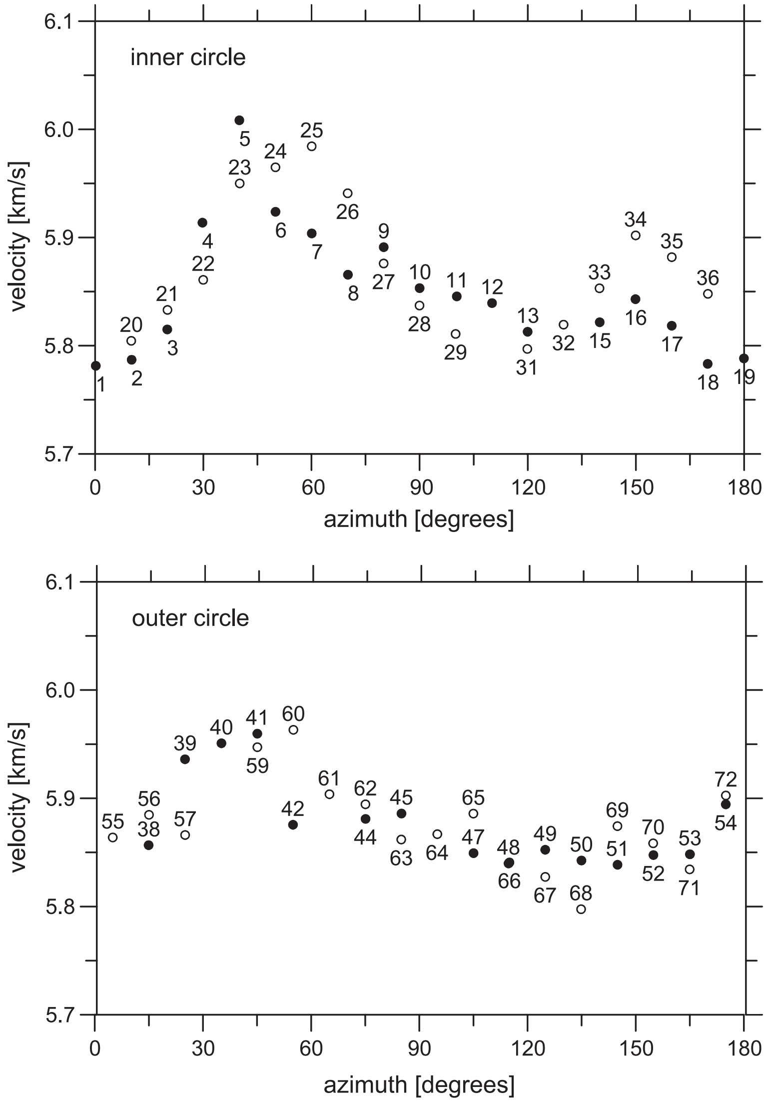

Fig. 9. Corrected *Pg* velocity as a function of azimuth for the inner (upper plot) and outer (lower plot) circles. Open/closed circles mark the stations in the azimuth range 0–180°/180–360°.

and the fluid-filled crack model in the directions parallel and perpendicular to the maximum compression. Obviously, these predictions clearly contradict our observations. This indicates that the observed anisotropy might be caused by preferred orientation of textural elements and minerals or large-scale fabrics imprinted in the crustal rocks during the early tectonic evolution rather than by aligned cracks or micro-cracks induced by the present-day tectonic stress in the region. The prevailing role of rock-fabric anisotropy is supported by coincidence of the fast direction of *Pg* waves with NE–SW trending of microstructural rock fabric in the part of the Moldanubian covered by the experiment (see Fig. 5). The NE–SW trending coincides with the direction of linear and planar structures in the Bohemian Massif attributed to the Variscan orogeny (Dallmeyer et al., 1995).

The domination of rock-fabric to crack-induced anisotropy is rather surprising, because usually the

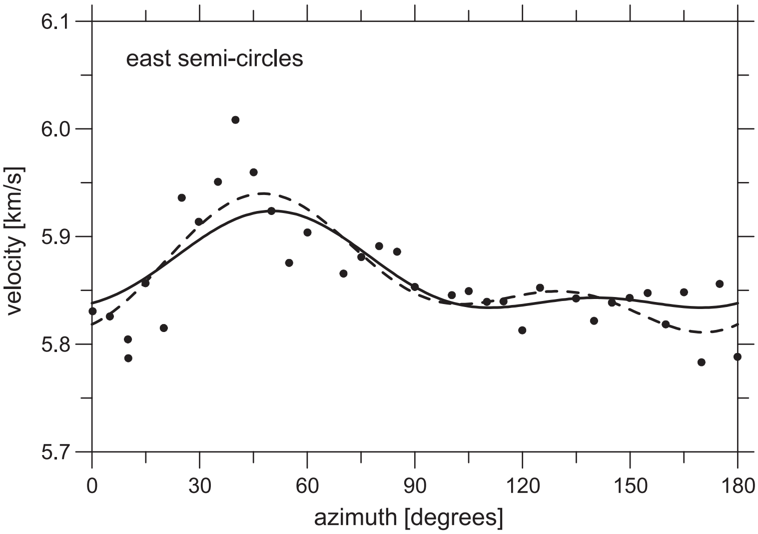

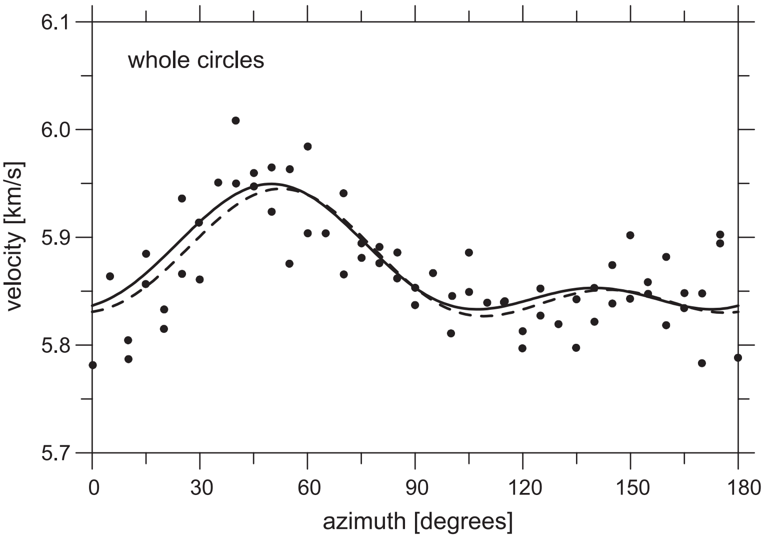

Fig. 10. Optimum anisotropy models. The azimuthal variation of the *Pg* velocity is shown for optimum weak anisotropy (dashed line) and weak transverse isotropy (solid line) models. The models are calculated from original travel times (marked by dots) measured along the east semicircles (upper plot) and from the corrected travel times measured along the whole circles.

crack-induced anisotropy in the uppermost crust is assumed to be at least as significant as the other types of anisotropy (Crampin, 1994; Rabbel, 1994; Rabbel and Mooney, 1996; Rasolofosaon et al., 2000). The minor contribution of the crack-induced anisotropy in the studied area might be explained by the presence of a small present-day deviatoric horizontal stress in the region. This would prevent a remarkable crack-induced anisotropy from developing. We can also speculate that cracks, oriented perpendicularly to rock foliation, affect the resultant velocity variation and cause its complex form (see Fig. 10). If so, the cracks should be water saturated and the strength of crack-induced anisotropy does not exceed 1%.

Interestingly, similar anisotropy values as found for the upper crust in the Moldanubian and in the entire Bohemian Massif (Růžek et al., 2003) have been detected also for the uppermost mantle studied by *Pn* waves. So far, the *Pn* anisotropy has not been studied in the Moldanubian part of the Bohemian Massif, but it was studied in the west from the Bohemian Massif. For example, Enderle et al. (1996) updated the interpretation of Bamford (1977) based on refraction experiments, and reported the *Pn* anisotropy of 3–4% immediately below the Moho with the maximum velocity in the direction N31°E. Song et al. (2001) studied the *Pn* anisotropy in the western part of the Bohemian Massif and in Germany using regional earthquakes and found anisotropy of 3.5–6% with the maximum velocity in the direction ~N25°E. Plenefisch et al. (1994) investigated 22 regional earthquakes in SW Germany and northern Switzerland and found anisotropy of 7% with the maximum velocity in the direction ~N50°E. The similar fast directions for the upper crustal and uppermost mantle anisotropy suggest a stable pattern of anisotropy orientation in the crust and the uppermost mantle in the Bohemian Massif and adjacent areas. This might indicate a common tectonic origin of crustal and uppermost mantle anisotropy. The anisotropy was probably induced by processes during Variscan orogeny when the Bohemian Massif was sandwiched between opposing subduction zones of NE–SW trending and when the preferential orientation of micro- and macrostructural fabrics was imprinted.

Acknowledgements

The authors thank H. Thybo and W. Rabbel for comments on the manuscript, and V. Babuška and V. Kachlík for discussions on the subject. This study was supported by Grant No. A3012309 of the Grant Agency AS CR, and by the CELEBRATION 2000 and ALP 2002 projects coordinated by A. Špičák and financed by the Ministry of Environment of the Czech Republic. The multi-azimuthal experiment was performed with the assistance of A. Boušková, J. Horálek, Z. Hudová, P. Jedlička, B. Růžek, J. Soukup, and J. Šílený. The TEXAN stations were provided by the University of Texas at El Paso, USA, and by the Polish Academy of Sciences. The assistance in station servicing and data downloading by Robert Pietrasiak is greatly appreciated.

References

Babuška, V., Cara, M., 1991. Seismic Anisotropy in the Earth. Kluwer Academic Publishing, London.

Backus, G.E., 1965. Possible forms of seismic anisotropy of the uppermost mantle under oceans. J. Geophys. Res. 70, 3429–3439.

Bamford, D., 1977. *Pn* velocity anisotropy in a continental upper mantle. Geophys. J. R. Astron. Soc. 49, 29–48.

Berckhemer, H., Rauen, A., Winter, H., Kern, H., Kontny, A., Lienert, M., Nover, G., Pohl, J., Popp, T., Schult, A., Zinke, J., Soffel, H.C., 1997. Petrophysical properties of the 9-km-deep crustal section at KTB. J. Geophys. Res. 102, 18337–18361.

Brudy, M., Zoback, M.D., Fuchs, K., Rummel, F., Baumgärtner, J., 1997. Estimation of the complete stress tensor to 8 km depth in the KTB scientific drill holes: implications for crustal strength. J. Geophys. Res. 102, 18453–18475.

Brückl, E., Bodoky, T., Hegedüs, E., Hrubcová, P., Gosar, A., Grad, M., Guterch, A., Hajnal, Z., Keller, G.R., Špičák, A., Sumanovac, F., Thybo, H., Weber, F., ALP 2002 Working Group, 2003. ALP 2002 seismic experiment. Stud. Geophys. Geod. 47, 671–679.

Chlupáčová, M., Skácelová, Z., Nehybka, V., 2003. *P*-wave anisotropy of rocks from the seismic area in western Bohemia. J. Geodyn. 35, 45–57.

Crampin, S., 1994. The fracture criticality of crustal rocks. Geophys. J. Int. 118, 428–438.

Dallmeyer, D., Franke, W., Weber, K., 1995. Pre-Permian Geology of Central and Eastern Europe. Springer-Verlag, New York.

Enderle, U., Mechie, J., Sobolev, S., Fuchs, K., 1996. Seismic anisotropy within the uppermost mantle of southern Germany. Geophys. J. Int. 125, 747–767.

Fusán, O., Kodym, O., Matějka, A., 1993. Geological map of the Czech Republic 1:1000000, uncovered. Czech Geological Survey.

Guterch, A., Grad, M., Keller, G.R., 2001. Seismologists celebrate the new millennium with an experiment in central Europe, EOS Trans. 82 American Geophysical Union 529, 534, 536.

Guterch, A., Grad, M., Keller, G.R., Posgay, K., Vozár, J., Špičák, A., Brückl, E., Hajnal, Z., Thybo, H., Selvi, O., CELEBRATION 2000 Working Group, 2003. CELEBRATION 2000 seismic experiment. Stud. Geophys. Geod. 47, 659–669.

Jahns, E., Rabbel, W., Siegesmund, S., 1996. Quantified seismic anisotropy at different scales: a case study from the KTB crustal segment. Z. Geol. Wiss. 24, 729–740.

Kaneshima, S., Ando, M., Kimura, S., 1988. Evidence from shear-wave splitting for the restriction of seismic anisotropy to the upper crust. Nature 335, 627–629.

Kern, H., Schmidt, R., 1990. Physical properties of KTB core samples at simulated in situ conditions. Sci. Drill. 1, 217–223.

Kern, H., Schmidt, R., Popp, T., 1991. The velocity and density structure of the 4000 m crustal segment at the KTB drilling site and their relationship to lithological and microstructural characteristics of the rocks: an experimental approach. Sci. Drill. 2, 130–145.

Málek, J., Brož, M., Fischer, T., Horálek, J., Hrubcová, P., Janský, J., Novotný, O., Růžek, B., 2001. Seismic measurements along short profiles in western Bohemia during the Celebration 2000 experiment. Acta Mont., Ser. A Geodyn. 18, 15–28.

Martínková, M., Pros, Z., Klíma, K., Lokajíček, T., Kotková, J., 2000. Experimentally determined *P*-wave velocity anisotropy for rocks related to the western Bohemia seismoactive region. Stud. Geophys. Geod. 44, 581–589.

Matte, Ph., Maluski, H., Rajlich, P., Franke, W., 1990. Terrane boundaries in the Bohemian Massif: result of large-scale Variscan shearing. Tectonophysics 177, 151–170.

Müller, B., Zoback, M.L., Fuchs, K., Mastin, L., Gregersen, S., Pavoni, N., Stephansson, O., Ljunggren, C., 1992. Regional patterns of tectonic stress in Europe. J. Geophys. Res. 97, 11783–11803.

Peška, P., 1992. Stress indications in the Bohemian Massif: reinterpretation of borehole televiewer data. Stud. Geophys. Geod. 36, 307–323.

Pitra, P., Burg, J.P., Guiraud, M., 1999. Late Variscan strike-slip tectonics between the Tepla-Barrandian and Moldanubian Terranes (Czech Bohemian Massif): petrostructural evidence. J. Geol. Soc. (Lond.) 156, 1003–1020.

Plenefisch, T., Faber, S., Bonjer, K.-P., 1994. Investigations of *Sn* and *Pn* phases in the area of the upper Rhine Graben and northern Switzerland. Geophys. J. Int. 119, 402–420.

Plomerová, J., Babuška, V., Ruprechtová, L., 1981. Travel times of seismic waves propagating to the Bohemian Massif from the South-West direction. Stud. Geophys. Geod. 25, 356–365.

Plomerová, J., Babuška, V., Ruprechtová, L., 1984. Velocities of seismic waves propagating through the Bohemian Massif from foci in Poland. Stud. Geophys. Geod. 28, 56–66.

Pros, Z., Lokajíček, T., Přikryl, R., Špičák, A., Vajdová, V., Klíma, K., 1998. Elastic parameters of West Bohemian granites under hydrostatic pressure. Pure Appl. Geophys. 151, 631–646.

Rabbel, W., 1994. Seismic anisotropy at the Continental Deep Drilling Site (Germany). Tectonophysics 232, 329–341.

Rabbel, W., Mooney, W.D., 1996. Seismic anisotropy of the crystalline crust: what does it tell us? Terra Nova 8, 16–21.

Rasolofosaon, P.N.J., Rabbel, W., Siegesmund, S., Vollbrecht, A., 2000. Characterization of crack distribution: fabric analysis versus ultrasonic inversion. Geophys. J. Int. 141, 413–424.

Růžek, B., Vavryčuk, V., Hrubcová, P., Zedník, J., the CELEBRATION Working Group, 2003. Crustal anisotropy in the Bohemian Massif, Czech Republic: observations based on Central European Lithospheric Experiment Based on Refraction (CELEBRATION) 2000. J. Geophys. Res. 108 (B8), 2392.

Schulmann, K., Plomerová, J., Babuška, V., Lexa, O., 2002. A kinematic model of the structural development of the Moldanubian root duing the Variscan orogeny based on correlation of crustal and mantle lithosphere fabrics. Geolines 14, 82–84.

Shearer, P.M., 1999. Introduction to Seismology. Cambridge Univ. Press, Cambridge.

Song, L.-P., Koch, M., Koch, K., Schlittenhardt, J., 2001. Isotropic and anisotropic *Pn* velocity inversion of regional earthquake traveltimes underneath Germany. Geophys. J. Int. 146, 795–800.

Vavryčuk, V., 1993. Crustal anisotropy from local observations of shear-wave splitting in West Bohemia, Czech Republic. Bull. Seismol. Soc. Am. 83, 1420–1441.

Vavryčuk, V., 1995. Reply to comments on "Crustal anisotropy from local observations of shear-wave splitting in West Bohemia, Czech Republic" by G.H.R. Bokelmann and J. Kawahara: Can the Hudson crack model describe behavior of real cracks? Bull. Seismol. Soc. Am. 85, 661–664.